

Scanning-tunneling-microscopy study of InSb(110)

L. J. Whitman, Joseph A. Stroscio, R. A. Dragoset, and R. J. Celotta
*Electron and Optical Physics Division, National Institute of Standards and Technology,
 Gaithersburg, Maryland 20899*

(Received 18 May 1990)

The (110) cleavage surface of InSb has been studied with scanning tunneling microscopy. A variety of surface defects has been observed, including those that appear to be simple vacancies and Schottky defects. Atomic-resolution images have been obtained of both the occupied- and unoccupied-state densities concentrated on the Sb anion and In cation, respectively. By simultaneously imaging both the occupied- and unoccupied-state densities, the relative positions of the In and Sb dangling bonds within the unit cell have been determined. As expected, the In state density is shifted with respect to the Sb state density by approximately one-half of a unit cell along the $[1\bar{1}0]$ direction. Along the $[001]$ direction, the In state density is displaced by approximately one-third of a unit cell, in good agreement with surface electronic structure and surface-buckling calculations. Measurements of the tunnel current versus voltage reveal conductance within the band gap associated with dopant-induced occupation of the conduction band.

The advent of scanning tunneling microscopy (STM) has led to the publication of atomic-resolution images of a wide variety of surfaces.¹ Although many studies of semiconductors have been reported, most have been of elemental Si surfaces.¹ To date, very few STM studies of clean III-V semiconductor surfaces reporting *atomic resolution* have been published; to our knowledge, only images of GaAs(110),^{2,3} GaAs(100),^{4,5} and GaAs(111) (Ref. 6) have appeared in the literature. This may be due to the relative difficulty of obtaining atomic-resolution images of these surfaces compared to elemental Si surfaces; lower tunnel currents must be employed and the surface-charge-density corrugations tend to be smaller.⁷

Application of the STM to the study of III-V compound semiconductors is particularly interesting on the (110) surfaces due to the polar nature of these materials. The two dangling bonds broken at the surface generally rehybridize into a single lone pair localized on the group-V element, leaving an empty valence orbital on the group-III element.⁸ Hence, the occupied-surface-state density, observed when tunneling from the sample to the tip, is concentrated on the group-V anion, and the unoccupied-state density, observed when tunneling from tip to sample, is on the group-III cation.⁹⁻¹¹ This enables atom-selective imaging of the different chemical elements on the surface,^{2,12} so that images acquired simultaneously of both filled- and empty-state densities may be used to infer the atomic positions of the constituent surface atoms, and thereby permit direct evaluation of calculated surface structures.²

In this Rapid Communication we report the structural and electronic properties of the (110) cleavage face of InSb as determined with STM. Although InSb is a narrow-band-gap semiconductor ($E_{\text{gap}} \approx 0.15$ eV) that has applications in near-infrared detection¹³ and high-speed electronics,¹⁴ relatively few studies of the surface properties of this material have been reported.¹⁵⁻²² As previously achieved with GaAs(110),² we have simultaneously

imaged the occupied- and unoccupied-state density associated with Sb and In, respectively. In addition, finite conductance within the band gap caused by dopant-induced conduction-band occupation has been observed in measurements of the voltage dependence of the tunnel current.

InSb(110)-oriented samples (*n*-type, Te-doped $1.6-3.0 \times 10^{15}$ cm⁻³) were cleaved *in situ* under ultrahigh vacuum ($< 1 \times 10^{-10}$ Torr) to expose a clean (110) crystal face, and immediately mounted on the STM. The STM is an IBM Zurich type microscope;^{23,24} the sample is mounted on a "louse" for coarse positioning, the tip is mounted on a piezotripod, and the whole microscope stage is mounted on a glass frame with a double-spring suspension system for vibration isolation. The probe tips were prepared by electrochemically etching (111)-oriented 0.005-in.-diameter tungsten wire, and cleaned *in situ* by electron-bombardment heating. Topographic images were obtained with a constant tunnel current of 0.1 nA, with a typical height resolution of 0.02 Å and lateral resolution less than 4 Å. Images recorded simultaneously at different bias voltages were obtained by completing one scan line at the first bias, returning the probe tip to the origin, and then switching the bias and recording another scan line at the second bias voltage. In this way the two images will be offset by at most the thermal drift that occurs during the scan of a single line, typically less than 0.1 Å. The images were recorded with the $[1\bar{1}0]$ direction at 45° with respect to the $+x$ scan direction. Those displayed here have not been corrected for the effects of thermal drift (typically $1-2$ Å min⁻¹).

After cleaving the samples *in vacuo*, (110) terraces with dimensions on the order of millimeters could usually be visually observed. Atomic-resolution images on such terraces frequently revealed large (a few-hundred-Å-wide) defect-free regions. Occasionally various surface defects are observed as illustrated in Figs. 1 and 2. The image displayed in Fig. 1 was obtained with a sample bias of

−2.5 V with respect to the tip, so that the occupied state density is observed. Since the occupied state density is concentrated on the anion, the image indicates the approximate positions of the Sb atoms. The known unit cell is 4.6 Å in the $[1\bar{1}0]$ direction and 6.5 Å in the $[001]$ direction, as indicated in the model of the surface on the bottom of Fig. 1. (Note that the unit cell in this image is slightly distorted by thermal drift.) The In atoms, whose occupied state density is not observed in the image, alternate with the Sb atoms along $[1\bar{1}0]$ and are predicted to be displaced from the Sb atoms by 1.4 Å in the $[001]$ direction.²⁵ Note that we have never observed any other ordered surface structures or reconstructions following cleavage.

The region of the surface imaged in Fig. 1 appears to have three vacancies. These defects appear as a simple absence of Sb state density, with little lateral perturbation of the surrounding dangling bonds. It also appears that the Sb row adjacent to the upper vacancy and the rows between the two lower vacancies are raised with respect to the neighboring rows (they appear brighter in the image). This may be due to some long-range electronic per-

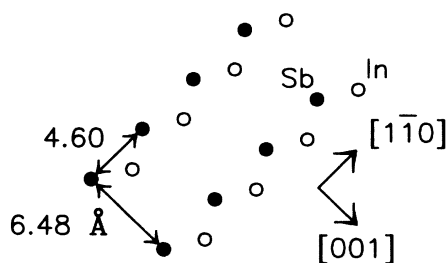
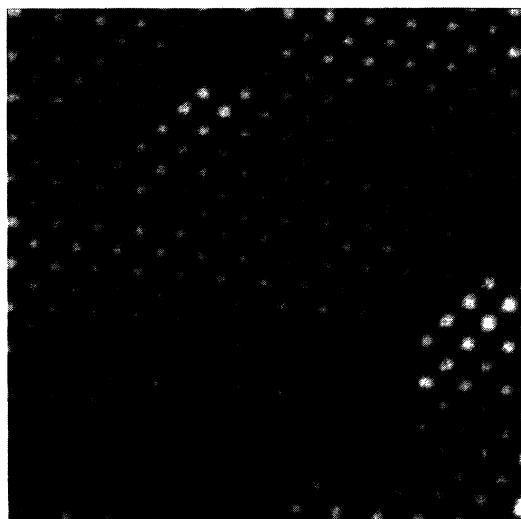


FIG. 1. A gray-scale STM image of a cleaved InSb(110) surface, approximately $100 \times 100 \text{ \AA}^2$. The image was acquired with a constant tunnel current of 0.1 nA and a sample bias of −2.5 V. The gray scale represents a height contrast of $\sim 1 \text{ \AA}$. Only the occupied state density, concentrated on the Sb atoms, is observed. The defects appear to be simple anion vacancies. A top-view model of the surface is also shown, with the uppermost In atom denoted by open circles and Sb denoted by solid circles. Note that the unit cell in this image is slightly distorted by thermal drift.



FIG. 2. A composite of two STM images of InSb(110) acquired simultaneously with sample biases of +1.5 V (unoccupied state density, in red) and −1.5 V (occupied state density, in blue). The area shown is approximately $30 \times 30 \text{ \AA}^2$. The relative positions of the empty and filled dangling bonds associated with the In (red) and Sb (blue) atoms, respectively, are apparent. The defect appears to be a Schottky defect, with adjacent Sb and In atoms missing.

turbations associated with the defect. Since images of similar defects acquired at positive sample bias show complete rows of In atoms, these defects appear to be simple anion vacancies. Although we cannot rule out the possibility that these features are adsorbate induced, we would expect more structure in and around the defects if that were the case.²⁶

A more complicated defect is evident in Fig. 2, where the Sb state density on another sample is shown in blue. The unoccupied state density, shown in red, has been imaged simultaneously for this topograph, revealing the relative positions of the empty orbitals associated with the In atoms. (The figure is a composite of the two images.) As in the defects discussed above, there appears to be an Sb vacancy; however, the composite image reveals that both an anion atom and the adjacent cation atom are not observed, i.e., this appears to be a Schottky defect.²⁷ The physical and electronic structure of these and other defects will be investigated more fully in future work.

The composite image shown in Fig. 2 also reveals the relative positions of the In and Sb state density. The In and Sb alternate along the rows in the $[1\bar{1}0]$ direction as expected. Along the $[001]$ direction the In state density is shifted in the Sb unit cell an amount determined by the surface buckling.² As shown in the model in Fig. 3, the (110) surface of III-V semiconductors relaxes with respect to the bulk-terminated structure, with the group-V element buckling outward and the group-III element inward.²⁵ For GaAs(110), which has been investigated more thoroughly, calculations show that the distance

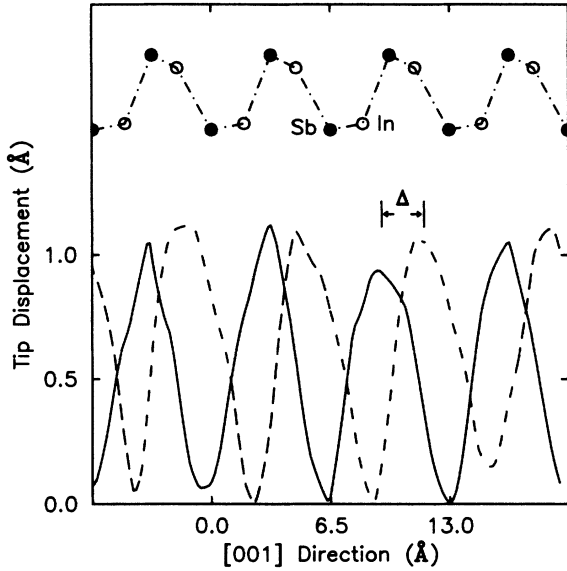


FIG. 3. A pair of STM profiles along the [001] direction of InSb(110) interpolated from two images acquired simultaneously at -1.5 (solid line; Sb, filled states) and $+1.35$ V (dashed line; In, empty states). The average displacement, Δ , of the Sb and In state density is 2.4 ± 0.4 Å. A side view of the atomic structure of the top two surface layers as calculated in Ref. 25 is shown for comparison (vertical dimensions not to scale).

along [001] between the filled and empty states, as observed in a STM topograph acquired with a tip-sample distance of 6 Å, increases from 1.2 Å when there is no buckling to 2.1 Å when the buckling angle is 30° (as defined by the III-V bond axis and the surface plane).² The InSb(110) surface structure (lattice constant $a_0 = 6.48$ Å) is very similar to that of GaAs(110) ($a_0 = 5.65$ Å); the relative positions of the filled and empty states should approximately scale with the lattice constant.²⁸ Hence, with a buckling angle of 30° , as calculated for InSb(110),²⁵ the In state density should appear shifted by 2.4 Å along [001] with respect to the adjacent Sb state density in STM topographs recorded with a tip-sample distance of 6 Å. In comparison, if there is no buckling a shift of only 1.4 Å should be observed.

A pair of profiles along the [001] direction interpolated from two images acquired simultaneously at -1.5 and $+1.35$ V is displayed in Fig. 3, showing clearly the relative displacements of the Sb-versus-In state density. Based on $I-V$ and $I-Z$ measurements, we estimate that the tip-sample distance at these voltages is 6 Å. We have measured the relative positions of the In and Sb state density along the [001] direction in this way in seven images obtained with three samples and tips, and sample biases at or near ± 1.5 V. The average separation $\Delta = 2.4 \pm 0.4$ Å (the uncertainty is one standard deviation), in excellent agreement with that expected on the basis of the calculated buckling. The large uncertainty reflects the fact that the tip shape and electronic structure, which will vary from tip to tip, can have a noticeable effect on the resulting image.

In addition to obtaining images of the InSb(110) sur-

face, we have also employed the scanning tunneling microscope to measure the tunnel-current-versus-voltage ($I-V$) characteristics. The $I-V$ characteristics were obtained by interrupting the STM feedback loop while holding the tip a fixed distance above the surface. $I-V$ curves were recorded with multiple, decreasing tip-surface distances in order to increase the dynamic range of the measurement in the region of the InSb band gap.³ A family of $I-V$ curves recorded in this way is shown in Fig. 4(a) for an initial sample bias of -1.5 V. It is difficult to resolve features near the band gap in a linear plot of the $I-V$ curves. The gap region can be more clearly observed, however, if the natural logarithm of the normalized current is displayed, as shown in Fig. 4(b). In this figure the tunnel currents have been normalized by taking into account the exponential dependence of the current on the tip-sample distance, $I \propto \exp(-2\kappa\Delta Z)$, where ΔZ is the relative tip-sample distance and κ is a function of the average barrier height.³ The expected positions of the

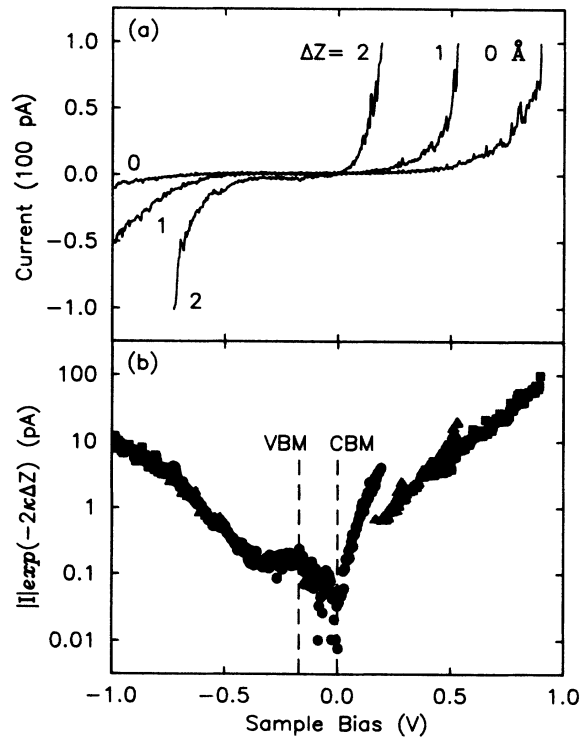


FIG. 4. (a) Tunnel-current-versus-voltage curves acquired with InSb(110) initially at -1.5 V ($I = 0.1$ nA) with the tip pushed closer to the sample an additional $\Delta Z = 1$ Å and $\Delta Z = 2$ Å. (b) Normalized tunnel-current-versus-voltage computed from the data in (a). The currents have been normalized by multiplying by $\exp(-2\kappa\Delta Z)$, where $\kappa = 0.8$ Å⁻¹. The dashed lines indicate the positions of the valence-band maximum (VBM) and conduction-band minimum (CBM) expected for n -type InSb (band gap ≈ 0.15 eV). The enhanced conductance near the VBM, including conductance in the expected band gap, is due to dopant-induced occupation of the conduction band. For each $I-V$ curve in (a), except that with $\Delta Z = 2$ Å, only data points above the noise level of the current amplifier are displayed. For $\Delta Z = 2$ Å, the current signal decreases below the noise level of the amplifier when the Fermi level is crossed near the CBM, causing the tunnel current to change direction.

valence-band maximum (VBM) and conduction-band minimum (CBM) for *n*-type InSb are indicated by the dashed lines in Fig. 4(b). When the sample bias is less than -0.5 V, tunneling out of occupied states in the valence band is observed. As the VBM is approached, however, additional tunneling occurs from states at the bottom of the conduction band occupied by dopant-induced carriers.³ This results in the enhanced conductance observed near the VBM. Tunneling from these dopant-induced states continues within the expected band gap of ≈ 0.15 eV until the Fermi level is crossed near the CBM, causing the tunnel current to reverse direction. (The current signal decreases below the noise level of the amplifier at this point.) For sample biases above the CBM, tunneling into unoccupied conduction-band states is observed. Note that in the absence of doping, tunneling would not occur within the band gap. These *I-V* curves, showing enhanced conductance around the VBM, including conductance within the band gap, are characteristic of degenerately doped *n*-type semiconductors.³

In summary, we have employed scanning tunneling microscopy to acquire atomic-resolution images of InSb(110) surfaces cleaved under ultrahigh vacuum. A variety of surface defects has been observed, including possible anion vacancies and Schottky defects. By simultaneously imaging the filled- and empty-state density, the empty dangling bond associated with each surface In atom is found to be shifted 2.4 ± 0.4 Å in the [001] direction with respect to the filled dangling bonds associated with the adjacent Sb atoms. This is in excellent agreement with the shift expected from the calculated surface buckling. In addition, by measuring the dependence of the tunnel current on sample bias voltage at decreasing fixed tip-sample distances, finite conductance within the band-gap characteristic of degenerately doped semiconductors has been observed.

We would like to thank S. Mielczarek and R. Cutkosky for expert technical assistance, and gratefully acknowledge the partial support of the Office of Naval Research.

- ¹For recent reviews, see C. F. Quate, *Phys. Today* **26**(8) (1986); P. K. Hansma and J. Tersoff, *J. Appl. Phys.* **61**, R1 (1987); G. K. Binnig and H. Rohrer, *Rev. Mod. Phys.* **59**, 615 (1987); Y. Kuk and P. J. Silverman, *Rev. Sci. Instrum.* **60**, 165 (1989). Also see Proceedings of the Fourth International Conference on Scanning Tunneling Microscopy/Spectroscopy [*J. Vac. Sci. Technol. A* **8**, 153 (1990)].
- ²R. M. Feenstra, Joseph A. Stroscio, J. Tersoff, and A. P. Fein, *Phys. Rev. Lett.* **58**, 1192 (1987).
- ³R. M. Feenstra and Joseph A. Stroscio, *J. Vac. Sci. Technol. B* **5**, 923 (1987).
- ⁴M. D. Pashley, K. W. Haberern, W. Friday, J. M. Woodall, and P. D. Kirchner, *Phys. Rev. Lett.* **60**, 2176 (1988).
- ⁵D. K. Biegelsen, L.-E. Swartz, and R. D. Bringans, *J. Vac. Sci. Technol. A* **8**, 280 (1990); D. K. Biegelsen, R. D. Bringans, J. E. Northrup, and L.-E. Swartz, *Phys. Rev. B* **41**, 5701 (1990).
- ⁶K. W. Haberern and M. D. Pashley, *Phys. Rev. B* **41**, 3226 (1990).
- ⁷Joseph A. Stroscio, R. M. Feenstra, D. M. Newns, and A. P. Fein, *J. Vac. Sci. Technol. A* **6**, 499 (1988).
- ⁸W. A. Goddard III, J. J. Barton, A. Redondo, and T. C. McGill, *J. Vac. Sci. Technol.* **15**, 1274 (1978).
- ⁹A. R. Lubinsky, C. B. Duke, B. W. Lee, and P. Mark, *Phys. Rev. Lett.* **36**, 1058 (1976).
- ¹⁰J. R. Chelikowski and M. L. Cohen, *Solid State Commun.* **29**, 267 (1979).
- ¹¹J. Tersoff and D. R. Hamann, *Phys. Rev. B* **31**, 805 (1985).
- ¹²J. Nogami, unpublished results.
- ¹³C. Y. Wei, K. I. Wang, E. A. Taft, J. M. Swab, M. D. Gibbons, W. E. Davern, and D. M. Brown, *IEEE Trans. Electron Dev.* **27**, 170 (1980).
- ¹⁴K. Asauskas, Z. Dobrovolskis, and A. Krotkus, *Fiz. Tekh. Poluprovodn.* **14**, 2323 (1980) [*Sov. Phys.—Semicond.* **14**, 1377 (1980)].
- ¹⁵C. B. Duke, R. J. Meyer, A. Paton, J. L. Yeh, J. C. Tsang, A. Kahn, and P. Mark, *J. Vac. Sci. Technol.* **17**, 501 (1980); R. J. Meyer, C. B. Duke, A. Paton, J. L. Yeh, J. C. Tsang, A. Kahn, and P. Mark, *Phys. Rev. B* **21**, 4740 (1980).
- ¹⁶J. Bohr, R. Feidenhans'l, M. Nielsen, M. Toney, R. L. Johnson, and I. K. Robinson, *Phys. Rev. Lett.* **54**, 1275 (1985).
- ¹⁷E. W. Kreutz, E. Rickus, and N. Sotnik, *Surf. Sci.* **151**, 52 (1985), and references therein.
- ¹⁸I. Hernández-Calderón, *Surf. Sci.* **152/153**, 1130 (1985); H. Höchst and I. Hernández-Calderón, *J. Vac. Sci. Technol. A* **3**, 911 (1985), and references therein.
- ¹⁹H. Lüth, *Surf. Sci.* **168**, 773 (1986), and references therein.
- ²⁰V. A. Grazhulis, *Appl. Surf. Sci.* **33/34**, 1 (1988).
- ²¹C. M. Aldao, I. M. Vitomirov, F. Xu, and J. H. Weaver, *Phys. Rev. B* **40**, 3711 (1989).
- ²²B. M. Trafas, C. M. Aldao, C. Capasso, Yoram Shapira, F. Boscherini, I. M. Vitomirov, and J. H. Weaver, *Phys. Rev. B* **40**, 9811 (1989).
- ²³G. Binnig and H. Rohrer, *Sci. Am.* **253**, 50 (1985).
- ²⁴R. D. Cutkosky, *Rev. Sci. Instrum.* **61**, 960 (1990).
- ²⁵C. Mailhot, C. B. Duke, and D. J. Chadi, *Surf. Sci.* **149**, 366 (1985).
- ²⁶Joseph A. Stroscio, R. M. Feenstra, and A. P. Fein, *Phys. Rev. Lett.* **58**, 1668 (1987).
- ²⁷See, for instance, R. Cotterill, *The Cambridge Guide to the Material World* (Cambridge University Press, Cambridge, 1985), p. 76.
- ²⁸J. Tersoff, private communication.

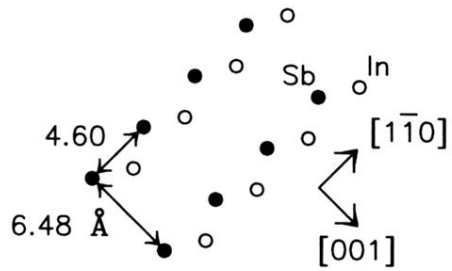
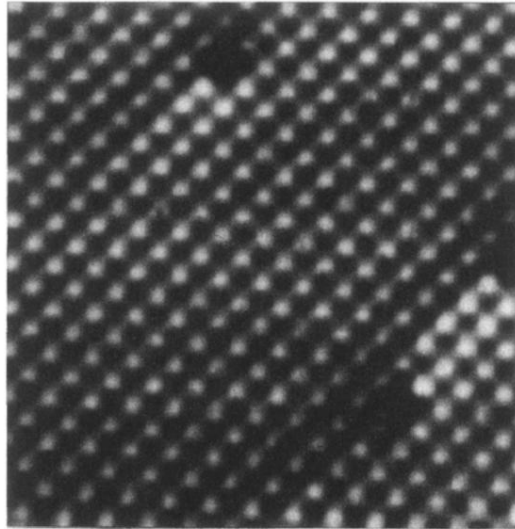


FIG. 1. A gray-scale STM image of a cleaved InSb(110) surface, approximately $100 \times 100 \text{ \AA}^2$. The image was acquired with a constant tunnel current of 0.1 nA and a sample bias of -2.5 V. The gray scale represents a height contrast of $\sim 1 \text{ \AA}$. Only the occupied state density, concentrated on the Sb atoms, is observed. The defects appear to be simple anion vacancies. A top-view model of the surface is also shown, with the uppermost In atom denoted by open circles and Sb denoted by solid circles. Note that the unit cell in this image is slightly distorted by thermal drift.

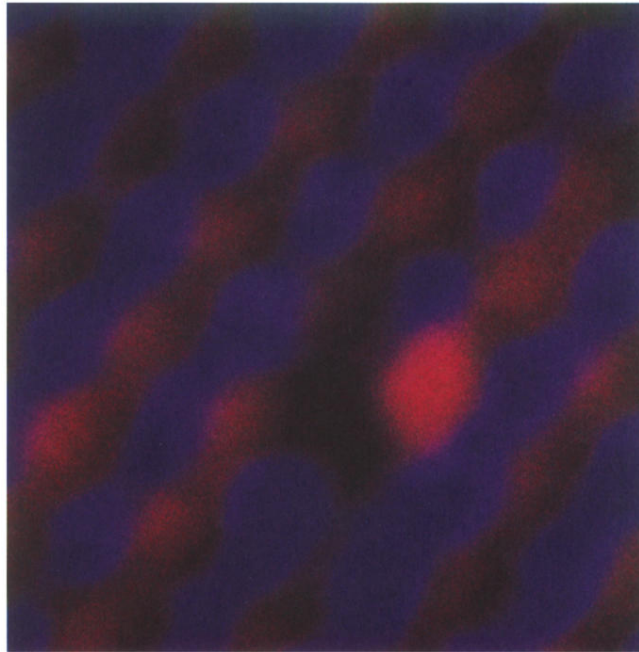


FIG. 2. A composite of two STM images of InSb(110) acquired simultaneously with sample biases of +1.5 V (unoccupied state density, in red) and -1.5 V (occupied state density, in blue). The area shown is approximately $30 \times 30 \text{ \AA}^2$. The relative positions of the empty and filled dangling bonds associated with the In (red) and Sb (blue) atoms, respectively, are apparent. The defect appears to be a Schottky defect, with adjacent Sb and In atoms missing.